

Article

A Novel Approach for Fabricating High-Performance Aluminum Matrix Composites: Friction Stir Processing with Micro-TiO₂ Particle Reinforcement by Grey-Taguchi Multi-Response Optimization

Suriya Prasomthong^{1,a}, Thanatep Phatunthane^{2,b}, and Chaiya Chomchalao^{1,c,*}

¹ Industrial Technology, Faculty of Industrial Technology, Nakhon Phanom University, 48000, Thailand

² Division of Science, Faculty of Education, Nakhon Phanom University, 48000, Thailand

E-mail: ^aSuriya.p@npu.ac.th, ^{b,*}p_thanatep@yahoo.com, ^{c,*}chaiwelding@ms.npu.ac.th (Corresponding author)

Abstract. The development of high-performance Aluminum Matrix Composites (AMCs) is critical due to the increasing demand for materials with superior mechanical properties, particularly in aerospace and automotive industries. This research addresses the need to enhance the hardness and impact energy of AA6061-T6 aluminum alloy by reinforcing it with micro-TiO₂ particles through Friction Stir Processing (FSP). The primary objective is to optimize the FSP parameters to improve these mechanical properties. A Grey-Taguchi method was employed for multi-response optimization, focusing on tool rotational speed, traverse speed, and TiO₂ particle volume. The methodology utilized Taguchi Orthogonal Arrays (OA) to minimize experimental runs while still capturing comprehensive data. Grey Relational Analysis (GRA) was applied to handle multiple correlated responses, converting them into a unified metric, the Grey Relational Grade (GRG). The results identified the optimal FSP parameters as a tool speed of 1100 rpm, traverse speed of 20 mm/min, and TiO₂ particle volume of 450 mm³, which significantly enhanced the mechanical properties. Comparative analysis revealed that the optimal parameters improved both hardness and impact energy by 15.80 J, with a GRG value of 0.905, indicating strong correlation between predicted and experimental outcomes. Confirmation experiments validated these results, with a 0.099 increase in GRG, suggesting that the combination of process parameters was highly effective. The findings highlight the significant influence of TiO₂ particle volume on the mechanical performance of the composite. These results provide critical insights to produce advanced AMCs, offering pathways to achieving high-performance materials for industrial applications.

Keywords: Aluminum matrix composites, FSP, Grey-Taguchi multi-response.

ENGINEERING JOURNAL Volume 29 Issue 1

Received 8 July 2024

Accepted 9 January 2025

Published 31 January 2025

Online at <https://engj.org/>

DOI:10.4186/ej.2025.29.1.27

1. Introduction

Aluminum and its alloys are widely utilized in diverse industries, including aerospace, automotive, energy, construction, and kitchenware [1–5]. Their extensive use is primarily attributed to three outstanding properties: low density, corrosion resistance, and favorable mechanical properties. Notably, aluminum and its alloys exhibit a superior strength-to-weight ratio compared to most engineering materials. These attributes have driven the scientific community to continuously develop novel aluminum alloys. However, the primary limitation of aluminum alloys lies in their inherent strength. To address this constraint, researchers have developed a multitude of alloy variations aimed at enhancing mechanical properties. The desired mechanical properties of existing aluminum alloys can be improved through various techniques, including microstructural modification [6], solid solution addition [7], heat treatments, casting, and friction stir processing (FSP). [8-10]

FSP is a promising technique for enhancing the mechanical properties of aluminum alloys while simultaneously mitigating casting defects and refining grain size [11]. Although research on the mechanical behavior of FSP-treated aluminum alloys is still nascent, it represents a compelling avenue for developing alloys with superior properties. The FSP process inherently improves mechanical properties through grain refinement. However, the incorporation of particles during the stirring process presents a further opportunity for property enhancement. These added particles can augment not only mechanical properties but also chemical and other characteristics. Nanosized particles, including both metallic and ceramic types, are frequently employed in FSP to develop novel alloys with enhanced mechanical properties [12]. Kumar C. S et al. [13] investigated the addition of tungsten particles to 5083 aluminum alloy, resulting in uniform particle distribution, reduced grain size, and increased mechanical properties. Notably, X-ray diffraction analysis revealed no metallic compound formation, and wear tests demonstrated improved wear resistance of the treated alloy surface. Khoshaim A. B et al. [14] explored the incorporation of graphene nanosheets (GNP), boron nitride (BN), and vanadium carbide (VC) into AA7075 aluminum alloy using FSP. The resulting composites exhibited a significant reduction in grain size, with a tenfold decrease compared to the base metal. Uniform particle distribution was achieved, and the AA7075/GNPs+BN+VC composite demonstrated the highest compressive strength and hardness values. However, the addition of GNP, BN, and VC reduced electrical conductivity by 7.3%, 24.4%, and 31.1%, respectively, while BN and VC also decreased thermal conductivity. Numerous other studies have investigated the effects of various particle additions on the properties of aluminum alloys through FSP [15-18]. These studies collectively underscore the potential of FSP as a versatile tool for tailoring the properties of aluminum alloys

through microstructural modification and particle reinforcement.

Among aluminum alloys, AA6061-T6 is renowned for its high strength and frequent use in automotive structures and chassis [19]. However, it exhibits limitations in terms of strength and hardness at elevated temperatures, susceptibility to galvanic corrosion, and wear resistance. Since thermal treatment cannot fully address these shortcomings [20], the incorporation of reinforcing materials, such as metal powder particles, presents an alternative avenue for achieving the desired properties. The Aluminum Matrix Composite (AMC) technique, utilizing the Friction Stir Processing (FSP) process, offers a reliable method for enhancing the properties of base materials by combining their attributes with the desirable characteristics of reinforcements. In this context, researchers have proposed the addition of titanium dioxide (TiO₂) particles to the surface of AA6061-T6 aluminum alloy using FSP. This study investigates the influence of production factors, including tool rotational speed, traverse speed, and TiO₂ particle volume, on the mechanical properties of the resulting composite. A Grey-based Taguchi method is employed for multi-response optimization, combining the robustness of Taguchi's experimental design with the flexibility of Grey Relational Analysis (GRA). This approach enables the simultaneous optimization of response variables, such as hardness and impact energy, by systematically varying the FSP parameters. By identifying the most suitable parameter combination, the desired properties of the AMC can be effectively achieved.

2. Literature Review

2.1. AMCs and Their Applications

Aluminum Matrix Composites (AMCs) combine aluminum as the matrix material with various reinforcements like fibers and particles to enhance mechanical properties such as strength, stiffness, and wear resistance. AMCs are widely applied in aerospace, automotive, and defense industries due to their lightweight and high-performance characteristics. Various studies have shown that composites with reinforcements like tungsten carbide exhibit superior mechanical properties, making them suitable for critical applications. Hybrid AMCs, which utilize combinations like ZrO₂ and B₄C, have demonstrated enhanced tensile strength and hardness compared to single-reinforcement composites [21-22]. The fabrication process, particularly stir casting, plays a crucial role in determining AMC properties. Stir casting is commonly used for large-scale production of AMCs, offering cost-effectiveness and flexibility in reinforcement selection. Applications of AMCs continue to grow, particularly in aerospace, where weight reduction of up to 20% improves fuel efficiency [23]. While significant progress has been made, challenges such as uniform reinforcement distribution and defect reduction remain. Future research aims to address these challenges,

optimize fabrication techniques, and ensure sustainable production for large-scale applications. AMCs hold great promise for industries requiring high strength, low weight, and resistance to extreme conditions.

2.2. FSP in Composite Fabrication

Friction Stir Processing (FSP) is a solid-state technique extensively used in metal-matrix composite fabrication. FSP refines microstructures and ensures uniform distribution of reinforcement particles, improving the mechanical properties such as hardness, strength, and wear resistance. Studies on Cu-SiC composites indicate that FSP enhances the microstructure and tribological properties, making it ideal for aerospace and automotive applications [24]. FSP is also highly effective in surface modification, improving surface properties while maintaining the material's bulk characteristics, especially in high-strength alloys like steel and titanium [25]. Additionally, friction stir welding (FSW), a variant of FSP, is superior to traditional fusion welding in joining composite materials, reducing defects like porosity, and strengthening the joints [26]. The integration of FSP with advanced technologies such as artificial intelligence and machine learning has enabled real-time quality monitoring during composite fabrication, improving the process's efficiency and reliability [27]. In conclusion, FSP offers a versatile and effective solution for producing high-performance composites, with continued advancements in hybrid processing and intelligent systems poised to push the boundaries of composite fabrication.

2.3. Role of Micro-TiO₂ Particles in Strengthening Aluminum Alloys

Micro-TiO₂ particles play a crucial role in enhancing the mechanical properties of aluminum alloys by promoting grain refinement and strengthening effects. Studies show that the inclusion of TiB₂ particles during processes like wire and arc additive manufacturing leads to a significant improvement in strength, with some aluminum composites exhibiting a 30% increase in strength [28]. These particles act as nucleation sites during the solidification of aluminum, refining the grain structure and enhancing overall material performance. Research on adding Ti particles to Mg AZ31/Al 6082 composite sheets also demonstrates improved tensile strength and elongation [29]. Ti (C, N) particles further enhance grain refinement, which leads to stronger, more durable composites compared to those reinforced with either Ti or TiCN alone [30]. Master alloys containing titanium and boron, such as Al₃Ti and TiB₂, are commonly used to refine grains in aluminum alloys, improving strength and wear resistance by inducing nucleation and reducing porosity during solidification [31]. The inclusion of micro-TiO₂ particles in aluminum alloys, therefore, presents a promising avenue for developing high-performance

materials for industries like aerospace and automotive, where enhanced strength and durability are critical.

2.4. Grey-Taguchi Method and Multi-Response Optimization in Composite Fabrication

The Grey-Taguchi method is a powerful approach for optimizing process parameters in composite fabrication, enabling multi-response optimization. By combining Grey Relational Analysis with the Taguchi method, this approach effectively handles multiple performance characteristics, making it suitable for complex optimization problems. The method has been applied to enhance the dimensional accuracy of parts fabricated through additive manufacturing processes like fused filament fabrication (FFF), resulting in improved precision of Polylactic Acid (PLA) parts [32]. It has also been employed in optimizing process parameters for fiber-reinforced polybutylene terephthalate (PBT) composites during injection molding, leading to enhanced wear resistance [33]. The versatility of the Grey-Taguchi method makes it suitable for various composite fabrication processes, including 3D printing and injection molding. By systematically optimizing multiple parameters, this method enhances material properties such as wear resistance, dimensional accuracy, and mechanical strength. Researchers continue to explore the method's potential in other composite manufacturing techniques, positioning it as an essential tool for achieving high-quality results in the production of advanced composite materials across multiple industries.

3. Experimental

3.1. Matrix Materials

The AA6061-T6 aluminum alloy comprises magnesium, silicon, copper, and trace amounts of other alloying elements, contributing to its strength and durability. The aluminum alloy AA6061-T6, boasting a strength of 285 MPa and hardness of 91 HV, is frequently utilized in the automotive sector. Its lightweight nature and impressive strength make it suitable for various components, including body panels, wheels, and chassis elements. Furthermore, it is utilized in the production of electric vehicle components, including body structures, chassis elements, suspension parts, motor housings, and battery casings. Additionally, it finds application in sporting equipment and electronic components. The mechanical and chemical properties are shown in Table 1 and Table 2, respectively.

Table 1. Chemical composition of AA6061-T6.

Materials	Element (%wt)							
	Al	Mg	Si	Fe	Cu	Zn	Ti	Mn
AA6061-T6	Bal.	0.82	0.47	0.27	0.07	0.18	0.05	0.12

Table 2. Mechanical properties of AA6061-T6.

Materials	Mechanical properties		
	F_u	F_y	H_V
AA6061-T6	285	237	91

3.2. Reinforced Particles

TiO₂, a versatile and ubiquitous material, finds extensive applications across various industries. Its notable properties contribute to its utility in diverse applications. For instance, its optical properties make it suitable for use in LED light-scattering products. Owing to its exceptional stability against chemical degradation, TiO₂ emerges as a favorable material for application as a surface layer on diverse substrates. Mechanically, TiO₂ can enhance strength and wear resistance, rendering it suitable for components subjected to abrasion. Furthermore, TiO₂ boasts additional desirable traits, including antibacterial, catalytic, and odor-absorbing capabilities. For this experiment, titanium dioxide with TiO₂ powder size of approximately 10 μm, which consists of 68.5 wt % titanium and 31.55 wt % oxygen, was used, as shown in Fig. 1.

3.3. Experimental Procedure

The FSP fabrication technique is employed in the production of AMC. This process is analogous to stirring the metal with a rotating tool under high heat input. The tool is plunged into the workpiece, inducing material agitation and softening, which allows the stirred zone to be shaped as desired. The production procedure for this study are as follows:

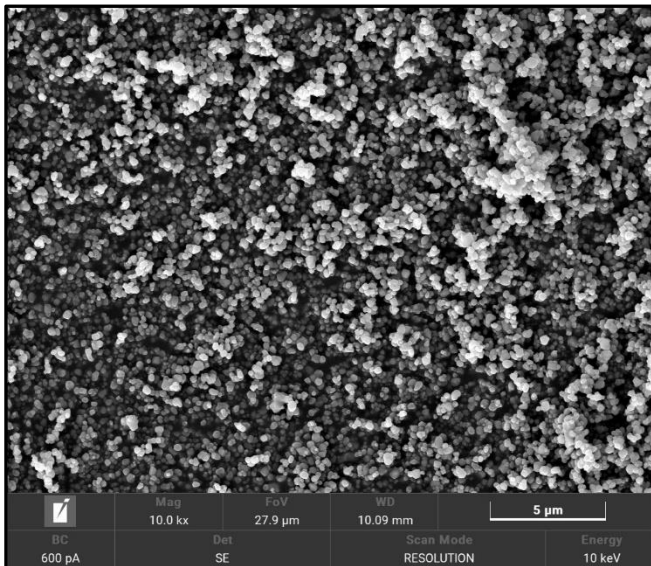


Fig. 1. The micro-TiO₂ Particle Reinforcement for experiment.

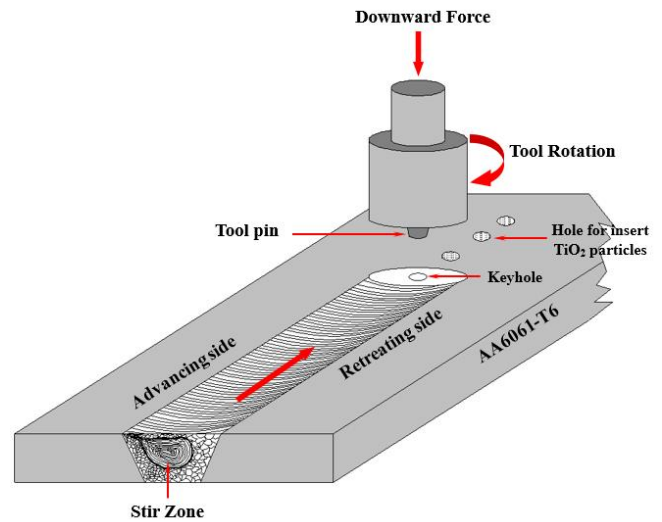


Fig. 2. Illustration of the tool configuration employed in the fabrication of AMC via the FSP process.

1. Experimental Setup: The fabrication of the AMC was conducted using a CNC machine (Model: VMC MACHINE CYCLONE-610) located at Nakhon Phanom University, Thailand. This machine facilitated precise control over the FSP parameters. The stirring tool, featuring a tapered threaded cylindrical profile, was fabricated from hardened SKD-11 steel, exhibiting a post-hardening hardness of 62 HRC. The experimental procedure for FSP is illustrated in Fig. 2.

2. Production Parameter Configuration: The production factors encompass tool rotational speeds, tool traverse speeds, and particle volume. The production parameters are outlined in Table 3.

3. Mechanical properties investigation: The mechanical properties testing protocol encompasses microhardness assessment in accordance with ASTM-E384 [34] and Charpy impact testing as per ASTM E23 [35]. Notably, the Charpy impact tests utilize subsize specimens, with dimensions illustrated in Fig. 3. The Charpy impact tests are conducted at room temperature.

Table 3. Parameters in AMCs fabrication using FSP process.

Parameter	Unit	Level		
		1	2	3
Tool speeds (S)	rpm	800	1100	1400
Travel speeds (F)	mm.min ⁻¹	20	40	60
Particle volume (PV)	mm ³	345	400	455

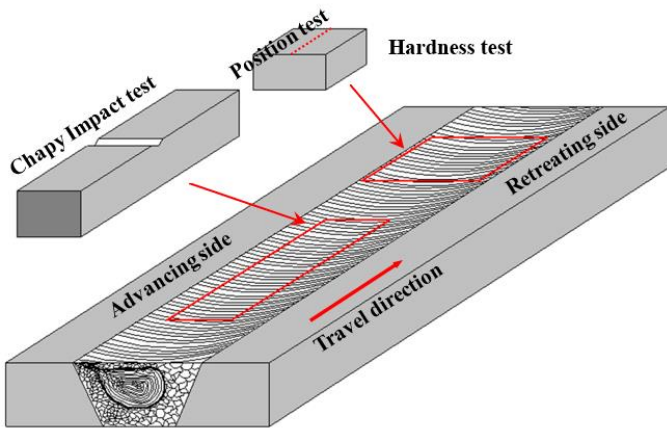


Fig. 3. Example of testing the mechanical properties of AMC using the FSP process.

4. Macro-Micro structure investigation: For macrostructural examination, samples fabricated through the FSP process were sectioned as illustrated in Fig. 2 and mounted in resin. The surfaces were polished sequentially using 80, 240, 400, 600, 800, and 1200 μm sandpaper, followed by cleaning with acetone and hot air drying. Etching was performed using a solution of 10 ml HF and 90 ml water for 20 seconds. Following the similar approach for macrostructural examination, the identical specimens were prepared for microstructural analysis. An additional polishing step, employing 0.5 μm alumina powder. Etching was then conducted using a solution of 2 ml HF, 3 ml HCl, 5 ml HNO_3 , and 190 ml water for 15 seconds, in accordance with ASTM E407 [36].

3.4. Experimental Design

This study employs a Grey-based Taguchi experimental design, a statistical methodology utilized to determine the optimal combination of multiple control factors for achieving the best possible outcomes across multiple response variables. This approach integrates Taguchi's robust experimental design principles with Grey Relational Analysis (GRA), a technique that effectively handles multiple correlated responses. The fundamental principles of the Grey-based Taguchi method are outlined as follows:

1. **Taguchi Orthogonal Arrays (OA)** are employed to minimize the number of experimental runs required while still yielding comprehensive data for analysis. The Taguchi method model is categorized into three distinct types: [37-40]

1.1) **Smaller-the-better:** This type is employed when the desired outcome is to minimize the value of the response variable. Examples include defects in welds, wear, surface roughness, etc. The Smaller-the-better model is represented by Eq. (1):

$$S / N_{\text{Smaller}} = -10 \log \sum_{i=1}^n \frac{y_i^2}{n} \quad (1)$$

1.2) **Larger-the-better:** This type is employed when the desired outcome is to maximize the value of the response variable. Examples include strength, product life, or mechanical properties. The Larger-the-better model is represented by Eq. (2):

$$S / N_{\text{Larger}} = -10 \log \sum_{i=1}^n \frac{1/y_i^2}{n} \quad (2)$$

1.3) **Nominal-the-best:** This type is employed when the desired outcome is for the response variable to be as close as possible to a specified target value. Examples include part dimensions, solution concentrations, and electrical resistance. In this scenario, the objective is neither to maximize nor minimize the response variable but to attain the closest proximity to the target value. This can be calculated as follows:

(1) Calculate the mean (T) of the experimental data:

$$T = \sum_{i=1}^n y_i$$

where n is the number of data points.

(2) Calculate the sum of squares of the mean (S_m):

$$S_m = T^2 / n$$

(3) Calculate the experimental variance (V_e):

$$V_e = \sum_{i=1}^n \frac{(y_i - T)^2}{n-1} = \frac{(y_1^2 + y_2^2 + \dots + y_n^2) - S_m}{n-1}$$

Therefore, the Nominal-the-best model is represented by Eq. (3):

$$S / N_{\text{Nominal}} = 10 \log \left[\frac{1}{n} \left[\frac{S_m - V_e}{V_e} \right] \right] \quad (3)$$

2. **Grey Relational Analysis (GRA)** is a statistical technique employed to analyze the relationships between factors when those relationships are obscure or complex. This method is particularly effective when dealing with "grey data," which refers to data that is uncertain, incomplete, or unclear. The procedural steps for conducting GRA are as follows:

2.1) **Normalization** is the transformation of raw data into dimensionless values within a specified range (typically 0 to 1) to facilitate comparison between datasets. To ensure comparability, the Signal-to-Noise (S/N) ratio of each experiment must be normalized. This involves converting the S/N ratios to a range between 0 and 1, where a higher S/N ratio (Larger-the-better) will have a value closer to 1, while a lower S/N ratio (Smaller-the-better) will have a value closer to 0. The normalization procedures for Larger-the-better, Smaller-the-Better, and Nominal-the-best are presented in Eq. (4), (5), and (6), respectively:[37]

$$Z_{ij} = \frac{y_{ij} - \min(y_{ij}, i = 1, 2, \dots, n)}{\max(y_{ij}, i = 1, 2, \dots, n) - \min(y_{ij}, i = 1, 2, \dots, n)} \quad (4)$$

$$Z_{ij} = \frac{\max(y_{ij}, i = 1, 2, \dots, n) - y_{ij}}{\max(y_{ij}, i = 1, 2, \dots, n) - \min(y_{ij}, i = 1, 2, \dots, n)} \quad (5)$$

$$Z_{ij} = \frac{(y_{ij} - T \arg et) - \min(|y_{ij} - T \arg et|, i = 1, 2, \dots, n)}{\max(|y_{ij} - T \arg et|, i = 1, 2, \dots, n) - \min(|y_{ij} - T \arg et|, i = 1, 2, \dots, n)} \quad (6)$$

2.2) The calculation of the Grey Relational Coefficient (GRC) is a crucial step in Grey Relational Analysis (GRA), serving to quantify the proximity or similarity between individual data sequences and a reference sequence representing the ideal outcome. The GRC measures the degree of relationship between the grey data sequences of response variables obtained from each experiment and the reference sequence. The GRC value ranges from 0 to 1, where a value of 1 signifies the highest degree of correlation between a data sequence and the reference sequence, while a value of 0 indicates the least correlation. The mathematical expression for calculating the GRC is presented in Eq. (7): [41]

$$\gamma(y_o(k), y_i(k)) = \frac{(\Delta \min + \xi \Delta \max)}{(\Delta_{oj}(k) + \xi \Delta \max)} \quad (7)$$

where:

1. j is the index of the experimental trial, ranging from 1 to n , where n is the total number of trials.
2. k is the index of the data point within a sequence, ranging from 1 to m .
3. $y_o(k)$ represents the reference sequence, where $y_j(k) = 1$ for all k .
4. $y_j(k)$ is a specific comparison sequence.
5. $\Delta_{oj} = \|y_o(k) - y_j(k)\|$ represents the absolute value of the difference between the reference sequence $y_o(k)$ and the comparison sequence $y_j(k)$.
6. $\Delta \min = \min_{\forall j \in i} \min_{\forall k} \|y_o(k) - y_j(k)\|$ is the smallest value among all $\Delta_{oj}(k)$ for a given comparison sequence $y_j(k)$.
7. $\Delta \max = \max_{\forall j \in i} \max_{\forall k} \|y_o(k) - y_j(k)\|$ is the largest value among all $\Delta_{oj}(k)$ for a given comparison sequence $y_j(k)$.
8. ξ is the distinguishing coefficient, a constant value between 0 and 1 used to adjust the sensitivity of the analysis. Typically, a median value of 0.5 is employed.

2.3) The Grey Relational Grade (GRG) is a metric used to analyze the relationships within data in Grey Relational Analysis (GRA), a multi-criteria decision-making method employed to address multi-objective problems. The GRG can be calculated using Eq. (8): [41]

$$\bar{\gamma}_j = \frac{1}{k} \sum_{i=1}^m \gamma_{ij} \quad (8)$$

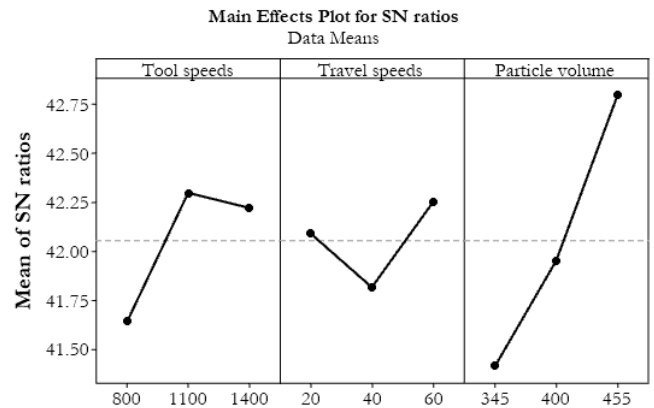
where $\bar{\gamma}_j$ is the Grey Relational Grade for experiment j and k performance feature, and m is the total number of performance features.

2.4) Following the identification of optimal FSP parameters, confirmatory experiments are conducted to validate the analysis. The anticipated GRG (γ_{pre}) can be calculated using the optimal parameter levels, as shown in Eq. (9): [41]

$$\gamma_{pre} = \gamma_m + \sum_{i=1}^q (\gamma_i - \gamma_m) \quad (9)$$

where γ_m is the total mean Grey relational grade (GRG).

γ_i is the mean GRG at the optimal level for each significant parameter. And q is the number of main parameters that significantly influence the overall quality characteristics.



Signal-to-noise: Larger is better

Fig. 4. Main effects plot for S/N ratio for Hardness test.

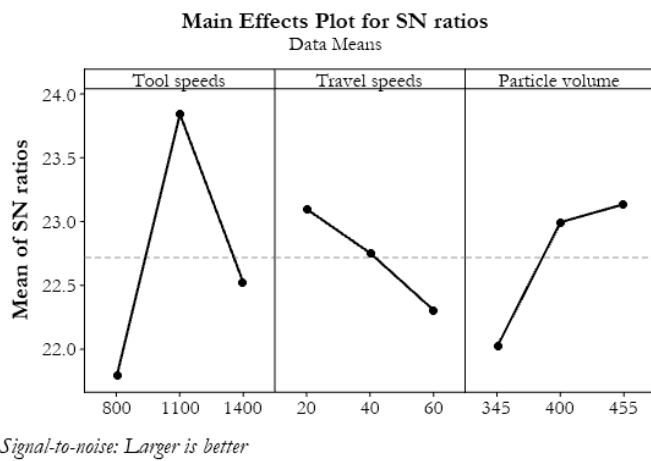


Fig. 5. Main effects plot for S/N ratio for Impact test.

4. Results and Discussion

4.1. Taguchi Analysis

Table 3 presents a Taguchi design of experiments (DOE) to investigate the effects of three control factors: Tool speeds (S), Travel speeds (F), and Particle volume (PV), on the response variables HV (Hardness Value) and Impact energy. The experiment consists of nine runs (No)

Table 3. Experimental results.

No.	S(rpm)	F (mm.min ⁻¹)	PV (mm ³)	HV	S/N for HV	Impact energy (J)	S/N for Impact energy (J)
1	800	20	345	113.76	41.1198	11.70	21.3637
2	800	40	400	116.98	41.3622	13.20	22.4115
3	800	60	455	132.51	42.4450	12.00	21.5836
4	1100	20	400	127.27	42.0945	16.40	24.2969
5	1100	40	455	138.60	42.8353	17.60	24.9103
6	1100	60	345	124.68	41.9159	14.20	23.0458
7	1400	20	455	142.31	43.0647	15.20	23.6369
8	1400	40	345	114.83	41.2011	12.10	21.6557
9	1400	60	400	131.87	42.4029	13.00	22.2789

Table 4. Analysis of Variance for SN ratios of hardness (HV).

Source	DF	Seq SS	Adj SS	Adj MS	F-value	P-value	Contribution%
S	2	0.74961	0.74961	0.37480	9.07	0.099	18.71
F	2	0.31933	0.31933	0.15967	3.86	0.206	7.97
PV	2	2.85408	2.85408	1.42704	34.52	0.028	71.25
Residual Error	2	0.08268	0.08268	0.04134			2.06
Total	8	4.00571					100.00

S = 0.2033; R-Sq = 97.94%; R-Sq_{adj} = 91.74%

Table 5. Analysis of Variance for SN ratios of impact energy (J).

Source	DF	Seq SS	Adj SS	Adj MS	F-value	P-value	Contribution%
S	2	8.2600	8.2600	4.1300	19.81	0.048	64.89
F	2	1.1214	1.1214	0.5607	2.69	0.271	8.81
PV	2	2.9305	2.9305	1.4653	7.03	0.125	23.02
Residual Error	2	0.4171	0.4171	0.2085			3.28
Total	8	12.7289					100.00

S = 0.4567; R-Sq = 96.72%; R-Sq_{adj} = 86.89%

based on an orthogonal array. The primary objective is to determine the optimal levels of S, F, and PV that maximize the desired outcome, as assessed by the S/N (Signal-to-Noise) ratio for both HV and Impact energy. The S/N ratio is advantageous as it considers the impact of both mean changes and variance in a single metric called mean square deviation (MSD), giving equal importance to both. A higher S/N ratio indicates better performance for a specific parameter combination. The experimental goal is to maximize both HV and Impact energy, thus a "Larger-the-Better" quality characteristic is considered. For this type of characteristic, the S/N ratio is calculated using Eq. (2). Table 3 results demonstrate the influence of the three control parameters on HV and Impact energy. To identify the factors significantly affecting the minimum variance in response, each response is converted into an S/N ratio, calculated using Eq. (2). Main effects plots for the S/N ratio are then generated for each of the three control parameters at their respective levels, as shown in Fig. 3 - 4. These plots reveal the optimal levels that maximize the response for each factor. Analysis of both graphs reveals a consistent influence of PV on both hardness and impact energy, demonstrating a positive correlation between PV values and S/N ratios. Conversely, S and F exhibit distinct effects on the S/N ratio in the hardness and impact tests, respectively.

Tables 3 - 4 illustrate the analysis of variance (ANOVA) results for the signal-to-noise (S/N) ratio derived from the Taguchi experimental design for hardness and impact energy, re-spectively. Table 4 reveals the contribution of each control factor (S, F, and PV) and residual error to the S/N ratio variation in the hardness test. Notably, PV emerges as the most influential factor, as evidenced by the highest F-value (34.52) and low P-value (0.028), suggesting sub-stantial impact of particle volume changes on hardness variability. S also exhibits a significant effect (F-value = 9.07, P-value = 0.099), while F demonstrates a lesser effect (F-value = 3.86, P-value = 0.206). The model accounts for 97.94% of the total S/N ratio variation (R-Sq), retaining 91.74% after adjustment (R-Sq_{adj}), with a residual standard deviation of 0.2033. Table 5 provides analogous information for the impact strength test. In this case, S is the most significant factor influencing the S/N ratio (F-value = 19.81, P-value = 0.048), followed by PV (F-value = 7.03, P-value = 0.125). F demonstrates the least impact (F-value = 2.69, P-value = 0.271). The model explains 96.72% of the total S/N ratio variation (R-Sq), reducing to 86.89% after adjustment (R-Sq_{adj}), with a residual standard deviation of 0.4567.

4.2. GRA Analysis

Table 3 presents the experimental results for the mechanical properties (hardness and impact energy) of

AMC fabricated using FSP with varying process parameters (*S*, *F*, and *PV*). The signal-to-noise (S/N) ratio was calculated for the response data to establish a reference sequence, utilizing the Larger-the-better criterion as defined in Equ. (2). Normalization, using Eq. (4), was then employed to transform the raw data into unitless values within the range of 0 to 1, ensuring equitable comparison across different factors. The deviation sequence, representing the absolute difference between the normalized data and the reference sequence, was subsequently calculated using Equation $\Delta_{oj} = \|y_o(k) - y_i(k)\|$. The grey relation coefficient (GRC), a measure of the relationship between each data point and the reference value, was computed based on the deviation sequence using Eq. (7). GRC values closer to 1 indicate a stronger relationship with the reference. Finally, the grey relational grade (GRG) was determined by averaging the GRCs for each factor, providing an overall assessment of the relationship between the dataset and the reference value. Higher GRG values, ranging from 0 to 1, signify a stronger overall relationship. The GRG was calculated using Eq. (8). The comprehensive results of these calculations are presented in Table 6.

Table 6. Normalization, deviation sequence, GRC and GRG of hardness and impact energy.

Exp. No.	Normalization		Deviation Sequence		Grey relation coefficient		GRG
	HV	Impact energy (J)	HV	Impact energy (J)	HV	Impact energy (J)	
1	0.000	0.000	1.000	1.000	0.333	0.333	0.333
2	0.125	0.295	0.875	0.705	0.364	0.415	0.389
3	0.681	0.062	0.319	0.938	0.611	0.348	0.479
4	0.501	0.827	0.499	0.173	0.501	0.743	0.622
5	0.882	1.000	0.118	0.000	0.809	1.000	0.905
6	0.409	0.474	0.591	0.526	0.458	0.487	0.473
7	1.000	0.641	0.000	0.359	1.000	0.582	0.791
8	0.042	0.082	0.958	0.918	0.343	0.353	0.348
9	0.660	0.258	0.340	0.742	0.595	0.403	0.499

Table 7. Response table for means of GRG.

Level	<i>S</i>	<i>F</i>	<i>PV</i>
1	0.4003	0.5820*	0.3847
2	0.6667*	0.5473	0.5033
3	0.5460	0.4837	0.7250*
Delta	0.2663	0.0983	0.3403
Rank	2	3	1

The experimental results presented in Table 6 indicate that experimental condition 5 (S2F2PV3) produced the highest values for both hardness (HV) and impact energy, with a GRG of 0.905. This GRG value, approaching 1, suggests that condition 5 is optimal for applications demanding both high hardness and impact resistance. Experimental condition 7 (S3F1PV3) yielded high hardness but moderate impact energy, making it suitable

for applications prioritizing hardness over impact resistance. Experimental conditions 3, 6, and 9 demonstrated moderate levels of both hardness and impact energy, rendering them suitable for general-purpose applications. In contrast, experimental conditions 2, 4, and 8 exhibited low values for both hardness and impact energy, indicating their unsuitability for applications requiring these properties.

Table 7 presents the results of the response analysis for mean GRG values at each level of the factors (S, F, and PV) used in AMC production via the FSP method. Optimal levels for achieving the highest GRG value are S2, F1, and PV3, suggesting that utilizing the second level of tool speed (S2), the first level of tool feed rate (F1), and the third level of particle addition quantity (PV3) yields the highest quality AMCs. Additionally, Delta and Rank values are employed to identify the factors most significantly influencing GRG. The Delta value, representing the difference between the highest and lowest GRG values for each factor, and the Rank, indicating the order of factors based on their Delta values, reveal PV as the most influential factor (Rank 1) with the highest Delta value (0.3403), followed by S (Rank 2) and F (Rank 3). Figure 6 illustrates the main effects plot for the mean of GRG.

Table 8 presents the ANOVA analysis results of the mean GRG values to assess the influence of various factors (S, F, and PV) on GRG, an indicator of the overall quality of the FSP process. The analysis shows that the PV factor significantly influences GRG, with an F-value of 12.24 and a P-value of 0.076, which is below the significance level of 0.05. This indicates that the variability of PV has a significant impact on the changes in GRG. Additionally, PV has the highest contribution percentage at 56.80%, indicating that PV is the most influential factor in optimizing the FSP process. Conversely, the factors S and F do not show a significant influence on GRG, with P-values of 0.121 and 0.495, respectively, both of which are above the significance level of 0.05. Although the S factor has a contribution percentage of 33.80%, it is still insufficient to conclude a significant impact on GRG. In summary, PV is the most critical factor in enhancing the efficiency of the FSP process and should be given special consideration in process design and control,

whereas the factors S and F may not require detailed adjustments to achieve optimal results.

Following the identification of optimal process parameters for the FSP process, a confirmation experiment was conducted to validate the accuracy of the predicted grey relational grade (γ_{pre}). Equation (9) was utilized to calculate the predicted grey relational grade under optimal conditions. Table 8 presents a comparison between the predicted and actual experimental values obtained using these optimal parameters, revealing a strong correlation. Furthermore, a significant improvement in both hardness and impact energy was observed after adjusting the initial parameters to their optimal values, with increases of 137.20 and 15.80, respectively. The data in Table 9 confirm a high degree of agreement between the predicted and actual grey relational grade values. Notably, the optimization of the initial parameters resulted in a 0.099 increase in the grey relational grade, suggesting a simultaneous enhancement of multiple performance characteristics, namely hardness and impact energy.

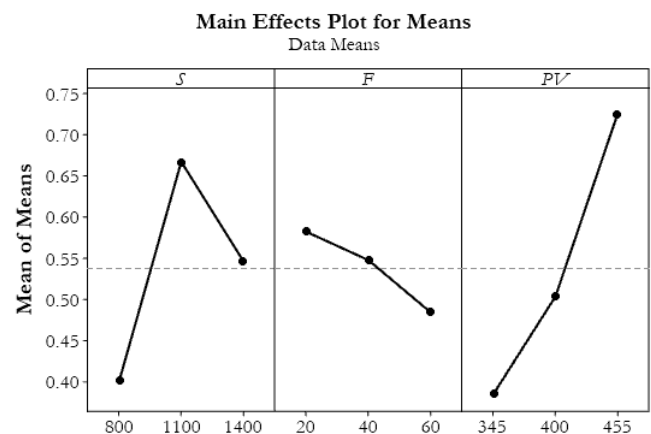


Fig. 6. Main effects plot for mean of GRG.

Table 8. Analysis of Variance for Means of GRG.

Source	DF	Seq SS	Adj SS	Adj MS	F-value	P-value	Contribution%
S	2	0.10671	0.10671	0.053356	7.30	0.121	33.80
F	2	0.01492	0.01492	0.007462	1.02	0.495	4.70
PV	2	0.17904	0.17904	0.089522	12.24	0.076	56.80
Residual Error	2	0.01462	0.01462	0.007312			4.16
Total	8	0.31531					100.00

S = 0.085; R-Sq = 95.36%; R-Sq(adj) = 81.45%

Table 9. Results of the confirmation experiments.

	Initial testing parameters	Optimal testing parameters	
		Prediction	Repeat the experiment
Parameter testing	S3F1PV3	S2F2PV3	S2F2PV3
Hardness (HV)	142.31		137.20
Impact energy (J)	15.20		15.80
GRG	0.791	0.8984	0.890

4.3. SEM Analysis

Figure 6 illustrates the chemical composition analysis of the S2, F2, PV3 sample surface, predicted and experimentally confirmed to exhibit optimal properties, using Energy Dispersive X-ray Spectroscopy (EDS). The primary SEM image reveals surface morphology, highlighting Position B, and the location of TiO_2 compounds. The EDS spectrum (I) at Position B indicates a predominance of Al, O, and Ti, suggesting the presence of TiO_2 , with trace amounts of Si, C, Cu, Mg, and Fe. In contrast, Fig. 7 depicts the S1, F1, PV1 sample, associated

with the lowest predicted performance. The EDS spectrum demonstrates a predominantly Al composition with reduced Ti content, alongside minor amounts of O, Si, C, Cu, Mg, and Fe. Collectively, Fig. 7 and 8 elucidate the distribution of TiO_2 compounds on the Ti/Al-based material surface. The presence of trace elements may be attributed to impurities or artifacts from sample preparation/analysis. The comparative analysis reveals a higher abundance of TiO_2 in S2, F2, PV3 than S1, F1, PV1, suggesting a significant influence of TiO_2 on the properties of friction stir processed aluminum matrix composites (AMCs).

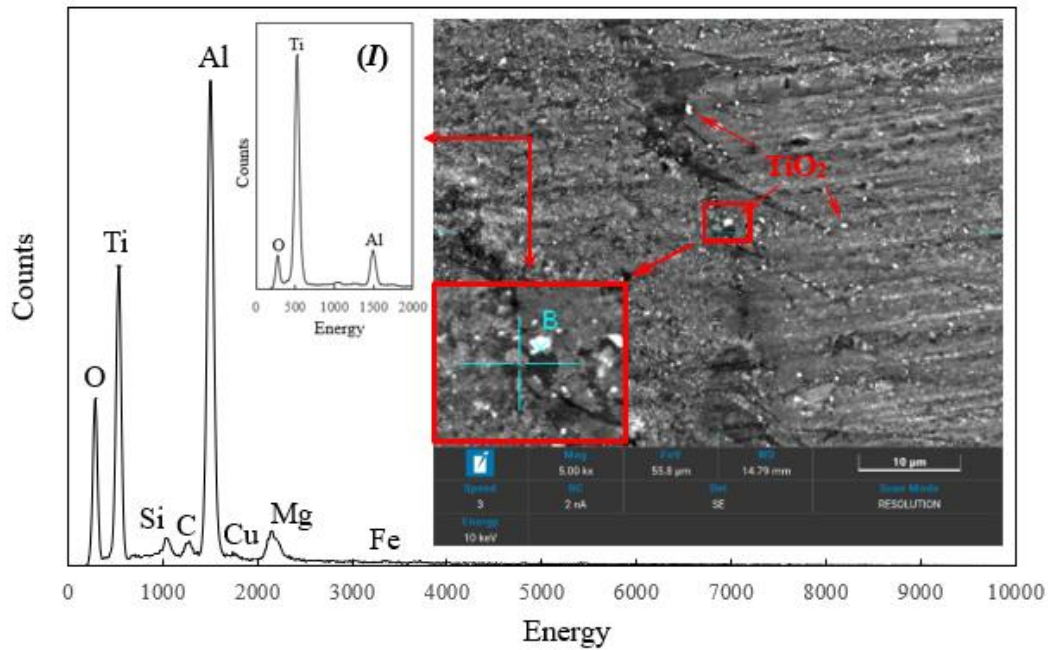


Fig. 7. Energy Dispersive X-ray Spectroscopy (EDS) of S2F2PV3.

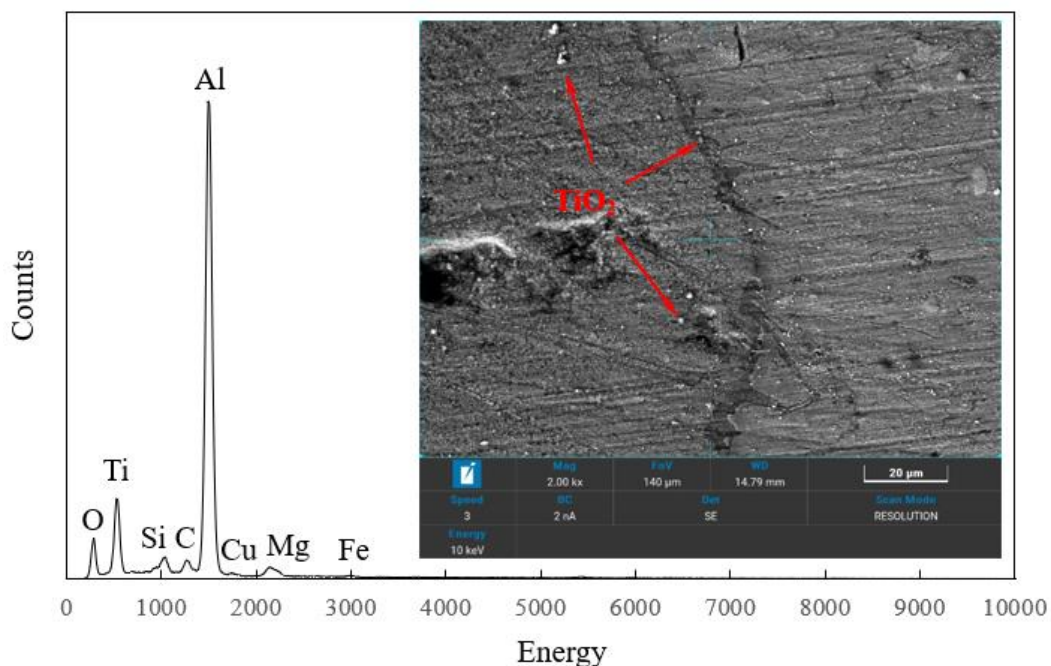


Fig. 8. Energy Dispersive X-ray Spectroscopy (EDS) of S1F1PV1.

Table 10 compares optimization methods for enhancing hardness (HV) and impact energy (J) of aluminum matrix composites (AMCs) reinforced with TiO₂ particles. Previous studies employed methods such as Grey-Taguchi, Taguchi-GRA, and Taguchi-Grey-TOPSIS, often reporting qualitative improvements without numerical values. For instance, [44] observed increased hardness and impact energy in Al7075-SiC composites but did not specify exact values. Similarly, [45] and [46] reported enhanced hardness for aluminum alloy composites but omitted impact energy measurements.

In contrast, this study reports precise outcomes: the Grey-Taguchi method optimized the hardness of AA6061-T6 reinforced with TiO₂ to 142.31 HV and the impact energy to 15.80 J. This highlights the method's strength in delivering quantifiable performance enhancements, addressing the limitations of prior works. These results demonstrate the efficacy of multi-response optimization in developing high-performance aluminum composites for advanced engineering applications requiring both strength and resilience.

Table 10. comparison method of Hardness (HV) and Impact energy (J) based on AMCs reinforced with TiO₂ particles.

References	Method	Material	Hardness (HV)	Impact energy (J)
[41]	Grey-Taguchi	General Aluminum MMCs	N/A	N/A
[42]	Grey-Taguchi L27	Hybrid Aluminum MMCs	N/A	N/A
[43]	Taguchi, Grey, TOPSIS	Aluminum Composites	N/A	N/A
[44]	GRA	Al7075-SiC Composite	Enhanced	Increased
[45]	Taguchi and GRA	Aluminum Alloy Composites	Enhanced	N/A
[46]	Taguchi- GRA	AA7075-TiO ₂	Improved	N/A
[47]	Taguchi-Based GRA	Hybrid Aluminum MMCs	Improved	N/A
This work	Grey-Taguchi	AA6061-T6 with TiO ₂	142.31 (optimized)	15.80 J (optimized)

5. Discussion

The application of the Grey-Taguchi method in optimizing the friction stir processing (FSP) parameters for aluminum matrix composites (AMCs) reinforced with TiO₂ particles demonstrates a significant improvement in mechanical properties. This method, known for its efficiency in multi-response optimization, allowed the research to focus on key FSP parameters such as tool rotational speed, traverse speed, and TiO₂ particle volume, identifying optimal conditions to enhance hardness and impact energy.

In this study, the reinforcement of AA6061-T6 aluminum alloy with micro-TiO₂ particles via FSP led to substantial increases in hardness and impact energy. This is primarily due to the refinement of the grain structure during the stirring process and the effective distribution of TiO₂ particles within the composite. The presence of micro-TiO₂ particles improved the composite's mechanical behavior by providing resistance to plastic deformation, which in turn increased hardness. The method also facilitated the production of a more homogenous composite, ensuring better load distribution during impact, thereby increasing impact energy. This finding aligns with prior studies that highlighted the benefits of using TiO₂ particles in aluminum composites, such as enhancing wear resistance and mechanical strength [8,9].

When compared to traditional FSP techniques, the use of the Grey-Taguchi method provided a systematic approach to optimizing multiple parameters simultaneously, resulting in a more efficient enhancement of mechanical properties. Previous studies, while

improving mechanical properties through FSP, often lacked the comprehensive optimization approach offered by Grey-Taguchi, which allowed for a more balanced improvement across multiple performance metrics [1]. The improvement in hardness and impact energy, as observed in this study, is higher than that achieved in similar studies involving different reinforcement materials like graphene nanosheets or tungsten particles. These materials, although effective in enhancing certain properties like compressive strength, did not achieve the same level of simultaneous improvement in both hardness and impact resistance as TiO₂ did when paired with the optimized FSP parameters [2,3].

The micro-TiO₂ particles played a critical role in enhancing the overall mechanical properties of the composite. The particles not only facilitated grain refinement but also acted as barriers to dislocation motion, thereby improving hardness. Their uniform dispersion within the aluminum matrix also contributed to increased impact energy by absorbing and redistributing the impact forces more effectively. This combination of particle reinforcement and optimized FSP parameters demonstrates the potential for developing high-performance AMCs tailored for demanding applications in the automotive and aerospace industries. The ability to produce materials with superior strength, hardness, and impact resistance is essential for these sectors, where weight reduction without sacrificing performance is a key requirement [10,12].

In summary, the Grey-Taguchi method proved highly effective in optimizing the FSP process for TiO₂ - reinforced AMCs, achieving a significant improvement in mechanical properties compared to traditional methods.

This approach paves the way for further advancements in the development of lightweight, high-performance materials for industrial applications. Future research could explore the use of nano-sized reinforcements or hybrid composites to push the boundaries of what can be achieved through this optimization technique [5,6]

6. Conclusions

The increasing demand for high-performance materials in the automotive and aerospace sectors necessitates advancements in the mechanical properties of aluminum alloys, particularly AA6061-T6, which is widely used due to its strength-to-weight ratio. However, its inherent limitations, such as insufficient hardness and impact resistance at elevated temperatures, require innovative reinforcement techniques. This research aimed to address these limitations by incorporating micro-TiO₂ particles into AA6061-T6 aluminum alloy via Friction Stir Processing (FSP) and optimizing the process parameters using the Grey-Taguchi method. The Grey-Taguchi multi-response optimization method was employed to identify the optimal FSP parameters tool rotational speed, traverse speed, and TiO₂ particle volume that would enhance both hardness and impact energy. Nine experimental runs were designed using Taguchi orthogonal arrays, and the results were analyzed using Grey Relational Analysis (GRA). The study revealed that the optimal FSP parameters 1100 rpm tool speed, 20 mm/min traverse speed, and 455 mm³ TiO₂ particle volume significantly improved the composite's hardness and impact energy. The confirmation experiments validated the findings, with an increase in both mechanical properties, demonstrating the effectiveness of the optimized parameters. Additionally, Energy Dispersive X-ray Spectroscopy (EDS) analysis confirmed the uniform distribution of TiO₂ particles on the material surface, contributing to the enhanced mechanical properties.

The implications of this research are significant for industries requiring advanced materials with enhanced durability, as the optimized process parameters enable the development of aluminum matrix composites (AMCs) with superior hardness and impact energy. This study demonstrates the utility of the Grey-Taguchi method for optimizing FSP processes, providing a robust framework for improving the performance of AMCs.

Future research could focus on exploring the influence of different types of reinforcement particles, such as nanoparticles or hybrid reinforcements, on the mechanical, thermal, and electrical properties of AMCs. Additionally, investigating the long-term performance of these composites under varying environmental conditions, such as high temperature or corrosive environments, would provide valuable insights for broader industrial applications.

Acknowledgement

I would like to express my heartfelt gratitude to my advisor, Dr. Chaiya Chomchalao, and Assistant Professor Dr. Somchat Sonasang for his unwavering support, invaluable guidance, and insightful advice throughout the course of my research and thesis writing. His expertise and dedication have been instrumental in the successful completion of this work. I would like to extend my sincere thanks to the Department of Industrial Technology, Faculty of Industrial Technology, Nakhon Phanom University, for providing the necessary resources, facilities, and a conducive environment for my research. The support from the department has been crucial in enabling me to pursue and complete my studies.

References

- [1] A. Silachai and S. Prasomthong, "Optimized parameter of dissimilar joining between Al6061-T6 and height-strength steel with friction stir spot welding process (FSSW)," *Journal of Metals, Materials and Minerals*, vol. 32, no. 4, pp. 118-127, 2022.
- [2] Y. Pookamnerd, P. Thosa, S. Charonerat, and S. Prasomthong, "Development of mechanical property prediction model and optimization for dissimilar aluminum alloy joints with the friction stir welding (FSW) process," *EUREKA: Physics and Engineering*, no. 3, pp. 112-128, 2023.
- [3] K. Harachai and S. Prasomthong, "Investigation of the optimal parameters for butt joints in a friction stir welding (FSW) process with dissimilar aluminium alloys," *Materials Research Express*, vol. 10, no. 2, p. 026514, 2023.
- [4] P. Luesak, R. Pitakaso, K. Sethanan, P. Golinska-Dawson, T. Srichok, and P. Chokanat, "Multi-objective modified differential evolution methods for the optimal parameters of aluminum friction stir welding processes of AA6061-T6 and AA5083-H112," *Metals*, vol. 13, no. 2, p. 252, 2023.
- [5] S. Patil, M. Nagamadhu, and T. Malyadri, "A critical review on microstructure and hardness of aluminum alloy 6061 joints obtained by friction stir welding-past, present, and its prospects," *Materials Today: Proceedings*, vol. 82, pp. 75-78, 2023.
- [6] F. Wang, J. Wei, G. Wu, M. Qie, and C. He, "Microstructural modification and enhanced mechanical properties of wire-arc additive manufactured 6061 aluminum alloy via interlayer friction stir processing," *Materials Letters*, vol. 342, p. 134312, 2023.
- [7] Ø. Ryen, B. Holmedal, O. Nijs, E. Nes, E. Sjölander, and H. E. Ekström, "Strengthening mechanisms in solid solution aluminum alloys," *Metallurgical and Materials Transactions A*, vol. 37, pp. 1999-2006, 2006.
- [8] S. P. Dwivedi, S. Sharma, C. Li, Y. Zhang, A. Kumar, R. Singh, and M. Abbas, "Effect of nano-TiO₂ particles addition on dissimilar AA2024 and AA2014 based composite developed by friction stir process

- technique,” *Journal of Materials Research and Technology*, vol. 26, pp. 1872-1881, 2023.
- [9] S. Sundaresan, S. Natarajan, S. Selvaraj, and C. Gopalsamy, “Mechanical properties of surface-modified magnesium alloy AZ61 with nanoparticles of aluminum oxide and titanium dioxide by friction stir processing,” *Hemijiska Industrija (Chemical Industry)*, 2023.
- [10] K. S. Sandhu, H. Singh, G. Singh, and H. Kishore, “Performance evaluation of additive TiO₂, MWCNT and GNP reinforced particles on Mg AZ31 based matrix composites by friction stir processing,” *Journal of Adhesion Science and Technology*, vol. 38, no. 5, pp. 637-653, 2024.
- [11] T. R. McNelley, “Friction stir processing (FSP): Refining microstructures and improving properties,” *Rev. Metal*, vol. 46, pp. 149-156, 2010.
- [12] B. Wu, M. Z. Ibrahim, S. Raja, F. Yusof, M. R. B. Muhamad, R. Huang, and S. Kamangar, “The influence of reinforcement particles friction stir processing on microstructure, mechanical properties, tribological and corrosion behaviors: A review,” *Journal of Materials Research and Technology*, vol. 20, pp. 1940-1975, 2022.
- [13] C. S. Kumar, R. Bauri, and D. Yadav, “Wear properties of 5083 Al–W surface composite fabricated by friction stir processing,” *Tribology International*, vol. 101, pp. 284-290, 2016.
- [14] A. B. Khoshaim, E. B. Moustafa, M. A. Alazwari, and M. A. Taha, “An investigation of the mechanical, thermal and electrical properties of an AA7075 alloy reinforced with hybrid ceramic nanoparticles using friction stir processing,” *Metals*, vol. 13, no. 1, p. 124, 2023.
- [15] N. Bharat and P. S. C. Bose, “Influence of nano-TiO₂ particles on the microstructure, mechanical and wear behaviour of AA7178 alloy matrix fabricated by stir casting technique,” *Proceedings of the Institution of Mechanical Engineers, Part L: Journal of Materials: Design and Applications*, vol. 237, no. 4, pp. 753-766, 2023.
- [16] K. J. Joshua, S. J. Vijay, and D. P. Selvaraj, “Effect of nano TiO₂ particles on microhardness and microstructural behavior of AA7068 metal matrix composites,” *Ceramics International*, vol. 44, no. 17, pp. 20774-20781, 2018.
- [17] M. Imran and A. A. Khan, “Characterization of Al-7075 metal matrix composites: A review,” *Journal of Materials Research and Technology*, vol. 8, no. 3, pp. 3347-3356, 2019.
- [18] M. A. Al-Jaafari, “Study the effects of titanium dioxide nano particles reinforcement on the mechanical properties of aluminum alloys composite,” in *IOP Conference Series: Materials Science and Engineering*, vol. 1105, no. 1, p. 012062, June 2021, IOP Publishing.
- [19] M. R. M. Aliha, M. Shahheidari, M. Bisadi, M. Akbari, and S. Hossain, “Mechanical and metallurgical properties of dissimilar AA6061-T6 and AA7277-T6 joint made by FSW technique,” *The International Journal of Advanced Manufacturing Technology*, vol. 86, pp. 2551-2565, 2016.
- [20] L. Li, E. A. Flores-Johnson, L. Shen, and G. Proust, “Effects of heat treatment and strain rate on the microstructure and mechanical properties of 6061 Al alloy,” *International Journal of Damage Mechanics*, vol. 25, no. 1, pp. 26-41, 2016.
- [21] E. C. Prasad Nidumolu, L. Yerra, and M. Baddepudi, “Study on the mechanical characteristics of aluminum metal matrix composites with tungsten carbide,” *Materials Today: Proceedings*, 2023.
- [22] K. Vijayalakshmi and G. B. Reddy, “Experimental study on mechanical properties of Al5083/ZrO₂/B₄C hybrid aluminum metal matrix composites,” *Materials Today: Proceedings*, vol. 80, pp. 1392-1396, 2023.
- [23] S. Dhanesh, K. S. Kumar, N. M. Fayiz, L. Yohannan, and R. Sujith, “Recent developments in hybrid aluminium metal matrix composites: A review,” *Materials Today: Proceedings*, vol. 45, pp. 1376-1381, 2021.
- [24] M. R. Akbarpour, H. M. Mirabad, F. Gazani, I. Khezri, A. A. Chadegani, A. Moeini, and H. S. Kim, “An overview of friction stir processing of Cu-SiC composites: Microstructural, mechanical, tribological, and electrical properties,” *Journal of Materials Research and Technology*, 2023.
- [25] A. Kumar and V. Kumar, “A review of recent progress in the fabrication of surface composites through friction stir processing,” *Materials Today: Proceedings*, vol. 63, pp. 494-503, 2022.
- [26] L. Zuo, X. Zhao, Z. Li, D. Zuo, and H. Wang, “A review of friction stir joining of SiCp/Al composites,” *Chinese Journal of Aeronautics*, vol. 33, no. 3, pp. 792-804, 2020.
- [27] R. Biradar and S. Patil, “A review of tensile, hardness, wear, and microstructural characteristics of friction stir welded/processed composites,” *Materials Today: Proceedings*, vol. 82, pp. 8-13, 2023.
- [28] H. Ren, Y. Liu, Q. Sun, P. Jin, Y. Tao, K. Kang, and Q. Sun, “Promoting strengthening and grain refinement of aluminum alloy during wire and arc additive manufacturing by adding TiB₂ particles,” *Materials Science and Engineering: A*, vol. 888, p. 145805, 2023.
- [29] X. Ai, Y. Dang, X. Jiang, X. Feng, R. Zhang, Y. Tian, and F. Pan, “The effect of Ti particles addition on the microstructure and mechanical behavior of Mg AZ31/Al 6082 composite sheets,” *Materials*, vol. 16, no. 7, p. 2844, 2023.
- [30] W. Li, J. Mao, and J. Feng, “Aluminium grain refinement by Ti(C, N) nanoparticles additions: Principles, advantages and drawbacks,” *Metallurgical Research & Technology*, vol. 116, no. 2, p. 212, 2019.
- [31] X. Wang, “Master alloys for grain refinement,” in *Encyclopedia of Aluminum and Its Alloys*. CRC Press, 2018, pp. 1417-1429.
- [32] K. E. Aslani, K. Kitsakis, J. D. Kechagias, N. M. Vaxevanidis, and D. E. Manolakos, “On the

- application of grey Taguchi method for benchmarking the dimensional accuracy of the PLA fused filament fabrication process,” *SN Applied Sciences*, vol. 2, pp. 1-11, 2020.
- [33] C. P. Fung, “Manufacturing process optimization for wear property of fiber-reinforced polybutylene terephthalate composites with grey relational analysis,” *Wear*, vol. 254, no. 3-4, pp. 298-306, 2003.
- [34] D. W. Hetzner, “Microindentation hardness testing of materials using ASTM E384,” *Microscopy and Microanalysis*, vol. 9, no. S02, pp. 708-709, 2003.
- [35] D. A. Fink, “Quantitative comparison and evaluation of various notch machining methods and how they affect ASTM E23 and ISO R442 testing equipment results,” *ASTM International*, 1990.
- [36] J. Ahuir Torres, “Microscopy techniques to analyse the characteristics of the metallic materials,” *Journal of Materials and Electronic Devices*, vol. 1, no. 1, pp. 33-53, 2023.
- [37] J. M. Cimbala, “Taguchi orthogonal arrays,” Pennsylvania State University, pp. 1-3, 2014.
- [38] A. Sunanta, W. Julsri, and S. Suranuntchai, “Optimization of forming process parameters for automotive advanced high strength steel parts using the Taguchi method,” *Engineering Journal*, vol. 28, no. 10, pp.25-46, 2024.
- [39] P. N. L. Pavani, R. P. Rao, and K. Santa Rao, “Performance assessment and mathematical modeling of process parameters in electrical discharge machining of EN-31 tool steel material using Taguchi DOE,” *Engineering Journal*, vol. 21, no. 2, pp. 227-236, 2017.
- [40] A. D. Prabowo, A. Amrizal, and G. A. Ibrahim, “Geometry optimization of PV/T-TEG collector under different operating conditions using CFD simulation and Taguchi method,” *Engineering Journal*, vol. 26, no. 8, pp. 1-11, 2022.
- [41] R. Siriyala, G. K. Alluru, R. M. R. Penmetsa, and M. Duraiselvam, “Application of grey-taguchi method for optimization of dry sliding wear properties of aluminum MMCs,” *Frontiers of Mechanical Engineering*, vol. 7, pp. 279-287, 2012.
- [42] P. P. Ikubanni, M. Oki, A. A. Adeleke, and O. O. Agboola, “Optimization of the tribological properties of hybrid reinforced aluminium matrix composites,” *Scientific African*, vol. 12, p. e00839, 2021.
- [43] S. Gajević, A. Marković, S. Milojević, A. Ašonja, and L. Ivanović, “Multi-objective optimization of tribological characteristics for aluminum composite using Taguchi Grey and TOPSIS approaches,” *Lubricants*, vol. 12, no. 5, pp. 171-180, 2024.
- [44] S. V. Gosavi and M. D. Jaybhaye, “Friction stir welding process optimization of Al 7075/SiC composites using Grey relational analysis,” *Materials Today: Proceedings*, vol. 72, pp. 719-723, 2023.
- [45] M. R. Shivakumar and M. K. Panchangam, “Multi-response optimization of reinforcement parameters of aluminum alloy composites by Taguchi Method and Grey relational analysis,” *Cell*, vol. 24, no. 2, pp. 223-237, 2024.
- [46] A. S. V., “Multi-objective optimisation of dry sliding wear control parameters for stir casted AA7075-TiO₂ composites using Taguchi-Grey relational approach,” *Australian Journal of Mechanical Engineering*, 2022, 20.5: 1453-1462.
- [47] S. Kumar and D. G. Mohan, “Simultaneous optimisation of multiple responses in end milling of aluminum hybrid composites using Taguchi-based Grey relational analysis,” *Advances in Materials Science and Engineering*, vol. 2024, 2024, Art. no. 6620348.



Suriya Prasomthong Currently pursuing a Doctor of Philosophy (Ph.D.) degree in Industrial Technology at the Faculty of Industrial Technology, Nakhon Phanom University. Previously earned a Bachelor of Engineering degree in Industrial Engineering (Production Engineering) from Rajamangala University of Technology Thanyaburi. Actively engaged in research investigating the optimal parameters for Friction Stir Processing using Grey-Taguchi Multi-Response.



Thanatep Phatungthane is currently an Assistant Professor in Division of Science at Faculty of Education, Nakhon Phanom University (NPU), Thailand. He received a B.Sc. in Physics, Maharakham University (MSU), Thailand, M.Sc. in Physics, Chiang Mai University (CMU), Thailand, and Ph.D. in Material Sciences, Chiang Mai University, Thailand. His research interests are Electroceramics, Dielectric Materials. Some of his recent articles have appeared in Current Applied Physics, Physical B: Condensed Matters and Journal of Electroceramics.



Chaiya Chomchalao earned his Ph.D. in Industrial Engineering from Ubon Ratchathani University in 2018. Additionally, he holds an M.Eng. in Industrial Engineering from Ubon Ratchathani University (2010) and a B.Eng. in Industrial Engineering from Pathumwan Institute of Technology (2002). Currently, Chaiya Chomchalao serves as a faculty member at the Faculty of Industrial Technology, Nakhon Phanom University. His research interests lie in transportation and supply chain management, focusing on enhancing efficiency and sustainability in transportation processes and supply chain management. His research aims to

contribute to the industrial sector and the broader economy.